tie-dyed1 Regulates Carbohydrate Accumulation in Maize Leaves[1][C][W][OA]

David M. Braun*, Yi Ma, Noriko Inada[2], Michael G. Muszynski[3], and R. Frank Baker

Department of Biology, Pennsylvania State University, University Park, Pennsylvania 16802 (D.M.B., Y.M., R.F.B.); Department of Plant and Microbial Biology, University of California, Berkeley, California 94720 (N.I.); and Department of Agronomic Traits, Pioneer Hi-Bred International, Inc., Johnston, Iowa 50131 (M.G.M.)

Acquisition of cell identity requires communication among neighboring cells. To dissect the genetic pathways regulating cell signaling in later leaf development, a screen was performed to identify mutants with chloroplast pigmentation sectors that violate cell lineage boundaries in maize (*Zea mays*) leaves. We have characterized a recessive mutant, *tie-dyed1* (*tdy1*), which develops stable, nonclonal variegated yellow and green leaf sectors. Sector formation requires high light, occurs during a limited developmental time, and is restricted to leaf blade tissue. Yellow *tdy1* sectors accumulate excessive soluble sugars and starch, whereas green sectors appear unaffected. Significantly, starch accumulation precedes chlorosis in cells that will become a yellow sector. Retention of carbohydrates in *tdy1* leaves is associated with a delay in reproductive maturity, decreased stature, and reduced yield. To explain the *tdy1* sectoring pattern, we propose a threshold model that incorporates the light requirement and the hyperaccumulation of photoassimilates. A possible function consistent with this model is that TDY1 acts as a sugar sensor to regulate an inducible sugar export pathway as leaves develop under high light conditions.

The maize (*Zea mays*) leaf has long been an attractive model system to study genes controlling leaf development and cell fate acquisition. It is a lanceolate organ divided into the distal blade and proximal sheath, which wraps around and connects the leaf to the stem. A large number of mutations perturbing various aspects of leaf development have been characterized (Freeling, 1992; Hall and Langdale, 1996). These have defined genes that act early in leaf development to specify regional fates and those that coordinate later spatial patterning events or final differentiation of specific cell types (Sylvester et al., 1990, 1996). Whereas mutational analysis and the cloning and characterization of the respective genes have elucidated many of the early leaf-patterning genes, much remains to be understood about the role cell-cell signaling plays in later leaf development.

Genetic studies using clonal mosaic analyses have revealed the clonal lineages comprising maize leaf development and determined that the orientations of cell divisions in growing leaf primordia are mostly transverse to the long axis of the leaf (Poethig, 1984; Poethig and Szymkowiak, 1995). These divisions produce linear cell files arranged in parallel to the long axis of leaves (Fig. 1A). Significantly, the great majority of investigations have found that cell identity is determined by a cell's final position within a leaf rather than its lineage (Sylvester et al., 1996), although exceptions exist (Jankovsky et al., 2001; Kessler et al., 2002). Hence, positional signals communicated from neighboring cells largely control acquisition of cell identity.

Maize uses C_4 carbon assimilation in leaf blade tissue, whereas other green tissues, such as sheath, utilize the C_3 pathway (Langdale and Nelson, 1991). The internal leaf tissue exhibits Kranz anatomy, with two distinct photosynthetic cell types arranged concentrically around the vascular tissue (Esau, 1977). Mesophyll cells surround bundle sheath cells, which in turn surround the vein. This anatomical arrangement reflects differences in physiological function. For example, almost all starch synthesis and accumulation occurs in the bundle sheath cells, but is largely absent from the mesophyll cells (Rhoades and Carvalho, 1944). Additionally, extensive grana stacking is seen in the mesophyll cell chloroplasts, whereas little or none is present in the bundle sheath cell thylakoid membranes (Kirchanksi, 1975).

To date, two genes responsible for specifying bundle sheath cell differentiation have been characterized.

[1] This work was supported by the National Research Initiative of the U.S. Department of Agriculture Cooperative State Research, Education and Extension Service (grant no. 2004–35304–14948 to D.M.B.).

[2] Present address: Nara Institute of Science and Technology, Plant Protein Biology, 8916–5, Takayama, Ikoma Nara 630–0101, Japan.

[3] Present address: Syngenta Seeds, Inc., Slater, IA 50244.

* Corresponding author; e-mail dbraun@psu.edu; fax 814–865–9131.

The author responsible for distribution of materials integral to the findings presented in this article in accordance with the policy described in the Instructions for Authors (www.plantphysiol.org) is: David M. Braun (dbraun@psu.edu).

[C] Some figures in this article are displayed in color online but in black and white in the print edition.

[W] The online version of this article contains Web-only data.

[OA] Open Access articles can be viewed online without a subscription.

www.plantphysiol.org/cgi/doi/10.1104/pp.106.090381

Figure 1. Clonal and nonclonal sectors in maize leaves. A, Arrow indicates clonal sector of white tissue illustrating longitudinal arrangement of cell files in a maize leaf. B, Variegated *tdy1* mutant leaf with yellow and green nonclonal sectors. C, *tdy1* leaf in anthocyanin-accumulating genetic background showing that yellow sectors accumulate red anthocyanins. White circle shows a regional island sector located adjacent to tissue of the opposite sector type. D, *tdy1* red sectors occur only in leaf blade tissues; leaf sheaths and husk leaf sheaths do not develop sectors. White arrow indicates a *tdy1* sector in leaf blade tissue at the tip of an ear husk leaf.

Both *bundle sheath defective2* (*bsd2*) and *golden2* (*g2*) mutants fail to accumulate the bundle sheath cell-specific enzyme Rubisco and have altered bundle sheath cell chloroplast ultrastructure (Langdale and Kidner, 1994; Roth et al., 1996). Neither mutant perturbs leaf blade mesophyll cell identity or function. Both genes were cloned from transposon-induced mutations that display somatic instability and reversion to wild-type function (Hall et al., 1998; Brutnell et al., 1999). Failure of the revertant wild-type sectors to restore function to the adjacent mutant tissue indicates that both BSD2 and G2 likely function cell autonomously and are not involved in communicating identity or function to nearby cells. Genes that coordinate a change in identity and physiological function at the whole-tissue level in leaves have not been identified.

To identify genes regulating cell fate among neighboring groups of cells, we screened for mutants that produce sectors that violate clonal lineage patterns in maize leaf development. We reasoned that sectors that cross lineage boundaries may result from a mobile signal transmitted between nonclonally related cells. For our screen, we utilized chloroplast pigmentation as an easily scorable marker to visualize nonclonal leaf sectors. In this article, we describe the isolation and characterization of *tie-dyed1* (*tdy1*), the first of a large group of mutants referred to as nonclonal-sectoring mutants. *tdy1* was isolated from an ethyl methanesulfonate (EMS)-mutagenized population and is inherited as a stable, nuclear recessive mutation that conditions variegated yellow and green leaf sectors. *tdy1* sectoring is restricted to a limited time in leaf development and is uniform throughout a sector, implicating cell signaling in sector formation. Additionally, sectors are irreversible and do not progressively expand in size. Whereas *tdy1* green sectors are essentially like wild-type tissue, *tdy1* yellow sectors display excessive accumulation of starch and soluble sugars within the photosynthetic cells, suggesting a defect in carbon export. Carbohydrate accumulation occurs prior to detection of a yellow sector, indicating that the down-regulation of chlorophyll levels (chlorosis) results from the hyperaccumulation of photoassimilates (Sheen, 1990). To our knowledge, no other mutant has been described that results in discretely variegated leaf sectors containing elevated levels of carbohydrates (Chatterjee et al., 1996; Keddie et al., 1996; Rodermel, 2002; Wang et al., 2004). Based on our investigations, a threshold model is proposed to explain the *tdy1* variegation and carbohydrate accumulation phenotypes.

RESULTS

tdy1 Is a Variegated Mutant Displaying Nonclonal Leaf Blade Sectors

To identify genes coordinating regional leaf identity, we screened for mutants with sectors that extend laterally beyond clonal lineages. Eight-hundred-forty EMS-mutagenized F_2 families were screened and a family was found to segregate plants with yellow- and green-pigmented leaf sectors that violate clonal lineage relationships (Fig. 1B). The sectors were stable in both shape and size over the lifespan of the leaves, with no reversion from green-pigmented to yellow-pigmented tissue or vice versa. Mutant leaves did not become necrotic or senesce any earlier than their wild-type siblings. Sectors often formed regional islands surrounded by the opposite sector type, demonstrating that the external environment alone does not condition a sector because cells adjacent to the sector developed in a nearly identical environment,

but formed the opposite sector type (Fig. 1C, circle). Additionally, formation of a yellow or green sector occurred coordinately over a region of tissue as evidenced by uniform pigmentation and lack of flecking, which would be expected to occur if each cell was independently sectoring. These data suggest that cell-cell signaling orchestrates sector formation in mutant leaves.

When the *tdy1* mutation was introduced into a genetic background capable of anthocyanin production in leaves, anthocyanins accumulated only in the *tdy1* yellow sectors (Fig. 1C). Hence, in this line, anthocyanins specifically mark *tdy1* yellow sectors. We analyzed *tdy1* plants throughout development to examine when and where sectors formed. Although the degree of sectoring per leaf varied, all leaves were capable of sectoring. Interestingly, *tdy1* yellow/red sectors manifested only in leaf tissue with blade identity, including reduced blade tissue at the tip of husk leaves, the specialized leaves that function to protect the ear (Fig. 1D). Sectors were not seen in leaf sheaths, in the sheaths of husk leaves, or on the stem, suggesting the *tdy1* defect specifically affects the leaf blade. Sectors could form anywhere in the blade, but with the greatest tendency to form in the tip and midregion, corresponding to the leaf areas receiving maximal incident light.

Because mutants displayed a variegated sectoring pattern reminiscent of the style of tie-dyed clothing, the mutation was named *tdy1*. To investigate the inheritance of the *tdy1* mutation, mutant plants were reciprocally crossed to standard inbred lines of maize. F_1 progeny were all wild type, indicating that the mutation is recessive and not maternally inherited through chloroplasts. F_1 plants were self fertilized to produce a F_2 generation that segregated 3:1 wild type:mutant (215 wild type:61 *tdy1*, χ^2 [3:1] = 1.24; $P = 0.27$), supporting monofactorial recessive inheritance. The *tdy1* locus was mapped to the long arm of chromosome six using a series of B-A translocations (Beckett, 1994). Hypoploid *tdy1*/− plants were phenotypically equivalent to the parental euploid *tdy1*/*tdy1* mutants. This suggests that the *tdy1* mutation is a genetic null mutation because there is no difference in phenotypic severity between one versus two mutant doses of the gene (Muller, 1932). Molecular markers were used to further fine map *tdy1*. *tdy1* resides between markers *umc1653* (approximately 0.3 cM proximal; one recombinant/320 chromosomes) and *asg7* (1.25 cM distal; four recombinants/320 chromosomes). Intriguingly, although *tdy1* is a stable recessive mutation and the gene product is defective in every cell, the phenotype is evident only in some portions of the leaf.

tdy1 Yellow Sectors Have Reduced Levels of Photosynthetic Pigments

tdy1 green sectors appeared similar to wild-type leaf tissue with the consequences of the *tdy1* mutation apparent only in the yellow tissue. To quantify the variation in pigmentation, we measured the amount of chlorophyll *a*/*b* and total carotenoids in mature leaves of *tdy1* yellow sectors, *tdy1* green sectors, and wild type (Table I; Supplemental Table S1). *tdy1* yellow sectors accumulated approximately 19% to 24% of chlorophyll *a*/*b*, and 34% to 40% of the total carotenoids compared to wild type. The pigment profile of *tdy1* green tissue was not significantly different from wild-type siblings. Hence, the *tdy1* mutant yellow sectors fail to accumulate photosynthetic pigments to the same level as the wild-type tissue, yet the green sectors appear equivalent to wild type.

High Light during a Limited Developmental Period Is Required for Sector Formation

Because chloroplast pigment accumulation is light regulated (Sestak, 1963) and dramatically reduced in *tdy1* yellow sectors, we hypothesized that light intensity plays a role in sector initiation. To test this hypothesis, a family segregating *tdy1* was grown under conditions of low or high light. Under a low light regime, *tdy1* and wild-type leaves did not sector (Fig. 2A). In contrast, *tdy1* leaves that developed under high light conditions produced sectors, whereas wild-type leaves showed no sectors (Fig. 2B). These results indicate a high light requirement for sector formation in *tdy1* leaves. Consistent with this finding, growing *tdy1* plants under constant high light produced strongly yellow-sectored leaves with a few green sectors restricted to leaf undulations and margins (Supplemental Fig. S1).

To examine the developmental competence of mutant plants to respond to a high light signal, we performed a light-shift experiment by transferring the low light-grown plants into the high light environment. After transfer, *tdy1* mutants produced new leaves that sectored (Fig. 2C). However, *tdy1* leaves that had matured in the low light environment did not sector. This experiment demonstrates that there is a

Table I. *Photosynthetic pigment quantification*

Data represent means from 12 samples ±SE, and the units are μg/g fresh weight.

Leaf Tissue	Chlorophyll *a*	% of Wild Type	Chlorophyll *b*	% of Wild Type	Total Carotenoids	% of Wild Type
Wild type	3,294.6 ± 82.0	100	714.9 ± 18.7	100	780.4 ± 23.6	100
tdy1 green	3,298.6 ± 69.4	100.1	689.3 ± 14.8	96.4	799.2 ± 14.8	102.4
tdy1 yellow	705.5[a] ± 20.1	21.4	141.6[a] ± 5.5	19.8	280.9[a] ± 8.0	36.0

[a]Value is significantly different from wild type at $P \leq 0.0001$ using Student's *t* test.

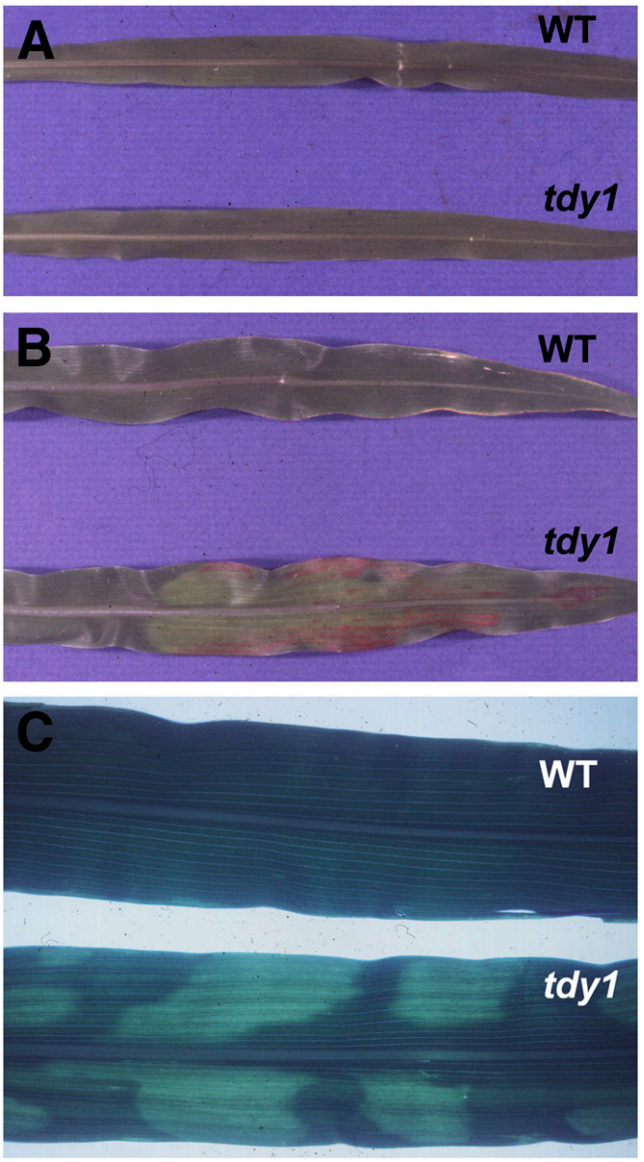

Figure 2. High light is required for *tdy1* sector formation. A, Plants grown in the low light treatment (75 μmol m^{-2} s^{-1} light). B, Plants grown in the high light treatment (1,400 μmol m^{-2} s^{-1} light). C, Subsequent leaves produced after plants were transferred from low to high light. WT, Wild type.

limited developmental time when sectoring is conditioned. Once past this time point, *tdy1* leaves are not competent to respond to the high light signal.

tdy1 Sectors Appear after Leaf Emergence

We monitored emerging *tdy1* leaves to investigate the timing and location of sector formation (Fig. 3). Day 1 was defined as the day the blade portion of a leaf was fully emerged from the whorl. Upon emergence and through day 4, the *tdy1* blade was a uniform pale green and showed no indication of sectoring (Fig. 3A). The first sign of sectoring was observed on day 5 as a region of tissue slightly paler than the neighboring light-green tissue (Fig. 3B). Ten days after emergence, the sector had become more evident against the darker green tissue background (Fig. 3C). The final form of the sector, as marked with anthocyanins, is shown on day 18 (Fig. 3D). Comparing the ultimate shape of the sector on day 18 with its shape on the day it is first visible, it can be seen that the boundary is unchanged (compare Fig. 3, B and D). This indicates that sectoring is not progressive, but occurs within a developmentally limited time frame.

tdy1 Yellow Sectors Hyperaccumulate Starch and Display Altered Cellular Ultrastructure

Because *tdy1* yellow sectors have decreased photosynthetic pigment levels compared to green sectors, we examined whether alterations in cellular and/or plastid morphology were present in mutant leaves. Wild-type and mutant tissue anatomy was visualized using 3,3′-dihexyloxacarbocyanine iodine ($DiOC_7$), a fluorescent dye that stains membranes, as well as by bright-field and UV illumination to inspect chlorophyll accumulation. Under UV illumination, chlorophyll autofluoresces a red color, whereas cell walls autofluoresce blue. In wild-type leaves stained with $DiOC_7$, mesophyll cells show bright-green fluorescence that corresponds to numerous chloroplasts with abundant photosynthetic membranes (Fig. 4A). Bundle sheath cells, with their less developed chloroplast membrane system, fluoresce less intensely, but also contain black precipitate indicative of starch grains (Fig. 4A). This precipitate is not observed in mesophyll cells. As seen with bright-field and UV illumination, chlorophyll is abundant in wild-type photosynthetic cells (Fig. 4, D and G). Photosynthetic

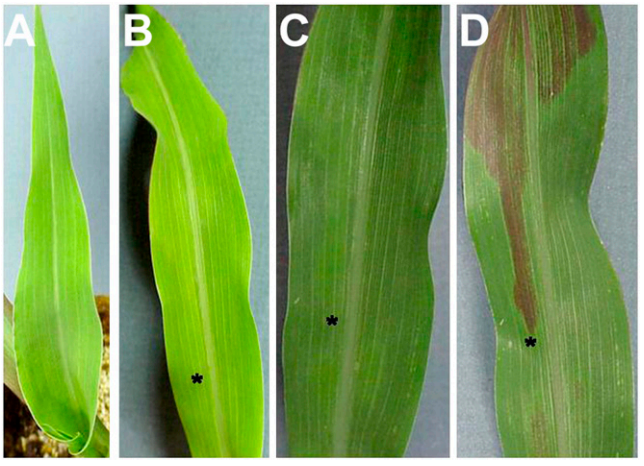

Figure 3. *tdy1* sectors are evident 5 d after leaf emergence from whorl. A, Day 1, blade portion of the leaf has fully emerged from the whorl. B, Day 5, faint yellow-green sector is visible. C, Day 10, the sector has a lighter olive-green coloration compared to neighboring green tissue. D, Day 18, the sector is marked by anthocyanin accumulation. Asterisks in B, C, and D mark the tip of the sector.

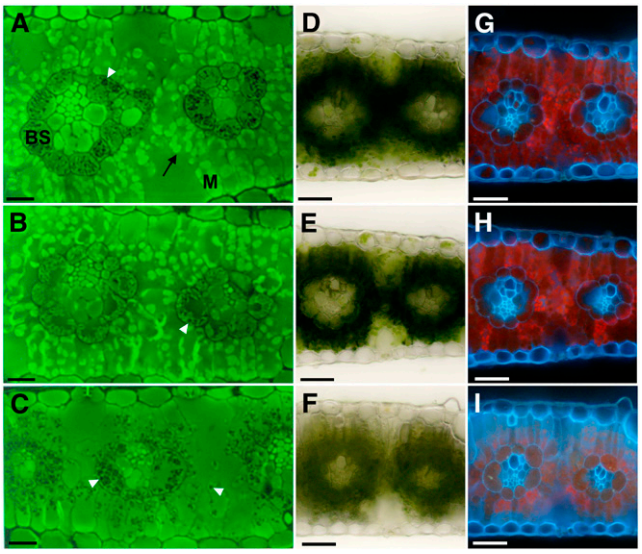

Figure 4. *tdy1* yellow sectors have reduced membrane staining and decreased chlorophyll autofluorescence. A to C, Fluorescent micrographs of cross sections of mature leaves stained with $DiOC_7$, a dye that stains membranes. White arrowheads indicate dark precipitate. A, Wild-type leaf. Bundle sheath (BS) cells surround the veins and mesophyll (M) cells surround the BS cells. Black arrow indicates intensely fluorescent mesophyll cell chloroplast. B, *tdy1* green sector likewise shows bright membrane staining in mesophyll chloroplasts. C, *tdy1* yellow sector displays greatly reduced membrane staining and abundant dark precipitates in both bundle sheath and mesophyll cells. D to F, Bright-field illumination of free-hand cross sections. G to I, UV illumination of free-hand cross sections. D and G, Wild type. E and H, *tdy1* green sector. F and I, *tdy1* yellow sector. Scale bars = 10 μm (A–C); 50 μm (D–I).

cells in green sectors from *tdy1* mutant leaves appear similar to wild type. Notably, mesophyll cells in green *tdy1* sectors display intense membrane staining equivalent to wild type and bundle sheath cells show the same dark precipitate (Fig. 4B). Additionally, chlorophyll abundance and autofluorescence in both photosynthetic cell types is comparable to wild type (Fig. 4, E and H). In contrast, yellow *tdy1* sectors exhibit strong reduction in membrane staining (Fig. 4C), chlorophyll accumulation, and autofluorescence (Fig. 4, F and I). Significantly, both mesophyll and bundle sheath cells in *tdy1* yellow sectors contain copious amounts of the dark precipitate, suggesting they accumulate excess starch (Fig. 4C).

To verify that the precipitate was starch and investigate the cellular ultrastructure, we examined wild-type and mutant photosynthetic cells using transmission electron microscopy (TEM). In mature wild-type leaves, mesophyll chloroplasts are round, have many grana membrane stacks, and accumulate little or no starch crystals, whereas bundle sheath chloroplasts are oblong, have few grana stacks, and accumulate multiple starch grains (Kirchanksi, 1975; Fig. 5A). Chloroplasts from leaves of *tdy1* green tissue appear similar to wild-type sibling tissue (Fig. 5B). However, in *tdy1* yellow sectors from the same leaf, both the mesophyll and bundle sheath chloroplasts accumulate large quantities of starch grains that occupy the vast majority of chloroplast volume (Fig. 5C). In mesophyll cells, almost no other organelles are discernible as the predominant vacuole appresses the chloroplasts and cytoplasm against the cell wall. Additionally, few grana stacks are visible in the chloroplasts. In bundle sheath cells, starch-packed chloroplasts are more round than oblong in shape and hardly any stroma can be seen. We conclude that the large excess of starch accumulating in mesophyll and bundle sheath chloroplasts of *tdy1* yellow sectors indeed corresponds to the dark precipitate observed in the fluorescent microscope (Fig. 4C).

tdy1 Yellow Sectors Accumulate Excess Carbohydrates Prior to Chlorosis

To test whether all photosynthetic cells in a yellow sector were accumulating high levels of starch, we qualitatively examined wild-type and *tdy1* sectored leaves by iodine staining (Fig. 6). We found that all cells throughout the yellow *tdy1* sectors stained strongly for starch accumulation (Fig. 6D). *tdy1* green sectors and wild-type tissue were weakly stained, indicating that these tissues contained far less starch (Fig. 6, B and D).

Because vacuoles are the temporary storage site for excess Suc transiently accumulated during daylight (Kaiser and Heber, 1984), we hypothesized that the predominant vacuoles visible in TEM images of *tdy1* yellow sectors may be due to elevated Suc accumulation in addition to excessive starch. To test this hypothesis, soluble sugar and starch concentrations within *tdy1* and wild-type leaves were quantified. As shown in Figure 7 and Supplemental Table S2, *tdy1* yellow sectors accumulated approximately 3 times as much Suc and approximately 10 to 16 times as much Glc, Fru, and starch as *tdy1* green sectors and wild-type leaves, whereas no significant differences were observed between green *tdy1* sectors and wild type. Hence, *tdy1* yellow sectors contain greatly increased amounts of carbohydrates.

High levels of photoassimilates are known to repress photosynthetic gene expression (Sheen, 1990) and therefore could be responsible for the yellow sectors in *tdy1* mutant leaves. Conversely, impaired plastid development could be the primary defect in *tdy1* yellow sectors and cause chlorosis, which in turn could lead to carbohydrate accumulation. To determine whether carbohydrate accumulation precedes visible sector formation, developing leaves were cleared of pigments and stained with iodine-potassium iodide (IKI) to detect starch. Emerging leaves were divided into thirds corresponding to the tip (oldest), middle, and base (youngest) regions. No region in wild-type leaves preferentially accumulated starch (Fig. 8, A and B). However, faintly visible yellow sectors in *tdy1* leaf tips already accumulated high levels of starch as shown by iodine staining (Fig. 8, C and D, arrows). The middle portion of the same leaf lacked visible sectors, yet differentially accumulated starch in cells

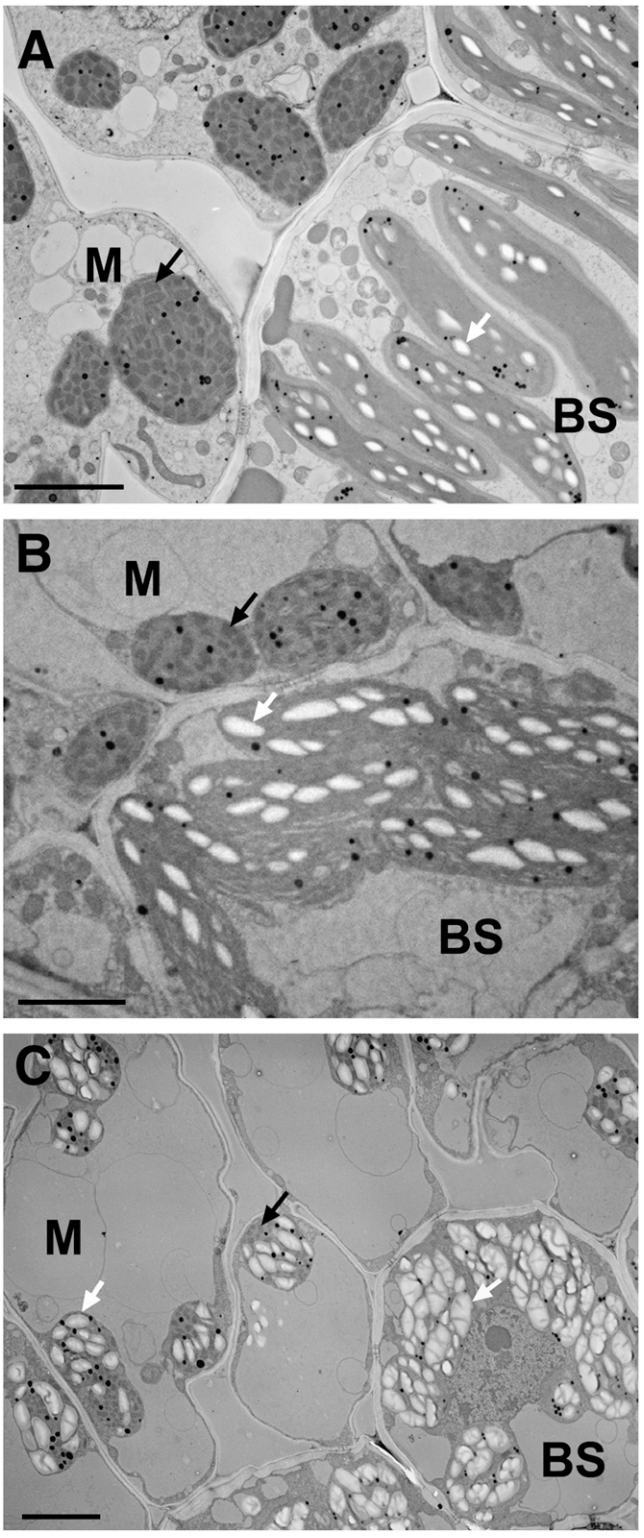

Figure 5. Photosynthetic cells in *tdy1* yellow sectors hyperaccumulate starch. TEM micrographs show ultrastructure of mesophyll (M) and bundle sheath (BS) cells. Starch grains are visible as white crystals inside chloroplasts indicated with white arrows. Black arrows show grana stacks in mesophyll chloroplasts. A, Wild-type leaf showing starch accumulation in BS cell chloroplasts, but no starch accumulation in M cell chloroplasts. B, *tdy1* green-leaf tissue showing starch accumulation in BS cell chloroplasts, but no starch in M cell chloroplasts. C, *tdy1* yellow sectors hyperaccumulate starch grains in both M and BS cell chloroplasts. Scale bars = 5 μm.

that would presumably become yellow sectors (Fig. 8, C and D, arrowhead). Finally, the base region of the blade just emerging from the whorl lacked visible sectors and preferential starch accumulation. Thus, excess carbohydrate accumulation occurs shortly after the tissue emerges from the whorl and prior to visible detection of a chlorotic sector in mutant leaves.

Reduced Rates of Photosynthesis and Gas Exchange in *tdy1* Yellow Sectors

The large accumulation of photoassimilates in *tdy1* yellow sectors was a surprising finding given the reduced photosynthetic pigment levels and the decreased chloroplast membrane abundance within *tdy1* yellow sectors (Table I; Fig. 4C). To test whether the yellow sectors could be directly synthesizing the carbohydrates present in these tissues, we investigated the rate of photosynthesis and gas exchange in mutant and wild-type leaves (Table II; Supplemental Table S3). Significantly, *tdy1* yellow sectors had approximately 16% of the photosynthetic rate of wild-type siblings, whereas green *tdy1* tissues had a photosynthetic rate similar to wild type. Most strikingly, yellow *tdy1* leaf sectors displayed approximately 3% of the stomatal conductance compared to wild-type leaves, whereas green sectors were not significantly different from wild type. Together, these results may suggest that the *tdy1* yellow sectors are not actively synthesizing the large amounts of carbohydrates present in these tissues.

Reduced Growth in *tdy1* Mutants

Because *tdy1* mutants have reduced rates of photosynthesis and contain elevated carbohydrate levels in leaves, we investigated whether plant growth and yield were affected in the mutant. Compared to wild type, plant height was reduced approximately 16% in *tdy1* mutants (Fig. 9A). In addition, a delay in reproductive maturity and a reduced inflorescence size were evident. Relative to wild type, anthesis in *tdy1* plants was delayed by 4 d and silk emergence by 5 d (Fig. 9B). Mutant tassels showed a dramatic 33% reduction in size (Fig. 9C) and branch length and number were also decreased (Supplemental Fig. S2). Last, *tdy1* ears were 20% shorter than wild type and kernel weight was reduced by 25% (Fig. 9D; Supplemental Fig. S3). These data suggest that retention of carbohydrates in *tdy1* leaves leads to retardation of growth and yield of mutant plants.

DISCUSSION

We have identified and characterized a nonclonal sectored mutant, *tdy1*, which causes large yellow- and

green-variegated sectors to form in leaf blades. *tdy1* sectors violate established cell lineage relationships in maize leaves. Thus, sector formation cannot be explained by a cellular inheritance-based mechanism, but must involve communication among cells, coordinating a decision to sector. This conclusion is drawn from the observation that all cells within a sector are uniformly pigmented. In addition, we frequently find islands of one sector type surrounding cells of the other sector type (Fig. 1C). These observations indicate that the external environment alone does not condition a sector because cells laterally adjacent, but of opposite sector type, experience nearly identical stimuli (light, temperature, CO_2 levels, etc.) as they develop. Instead, these data suggest that an endogenous signal is at least partly responsible for orchestrating sector formation. As elaborated below, we propose that Suc is a candidate for this endogenous signal.

The external environment plays an important role in *tdy1* sectoring, however, because we found that it is strongly influenced by the light environment. Induction of sectoring does not occur under a low light regime, but requires high light (Fig. 2, A and B). A possible explanation is that high light is necessary to produce the endogenous signal that is communicated among neighboring groups of cells and determines their fate. Production of high levels of photoassimilates occurs in high light and is consistent with the proposed role for Suc as the signal. Further, light-shift experiments revealed that there is a limited time during leaf development when high light induces sector formation. We observed that leaves that matured in the low light environment failed to form sectors when shifted to the high light environment and, hence, had passed this time point in their development. This conclusion is also supported by the fact that green sectors of mature, field-grown *tdy1* leaves that are repeatedly exposed to daily high light levels

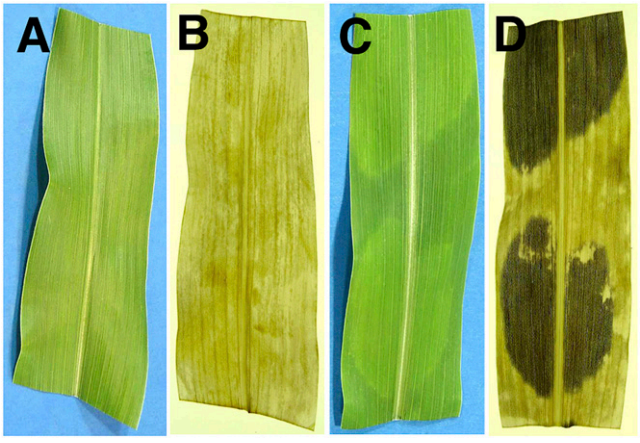

Figure 6. *tdy1* yellow sectors accumulate starch throughout the sectors. A and B, Wild-type leaf. C and D, *tdy1*-sectored leaf. A and C, Photographs before staining. B and D, Photographs of cleared, IKI-stained leaves. [See online article for color version of this figure.]

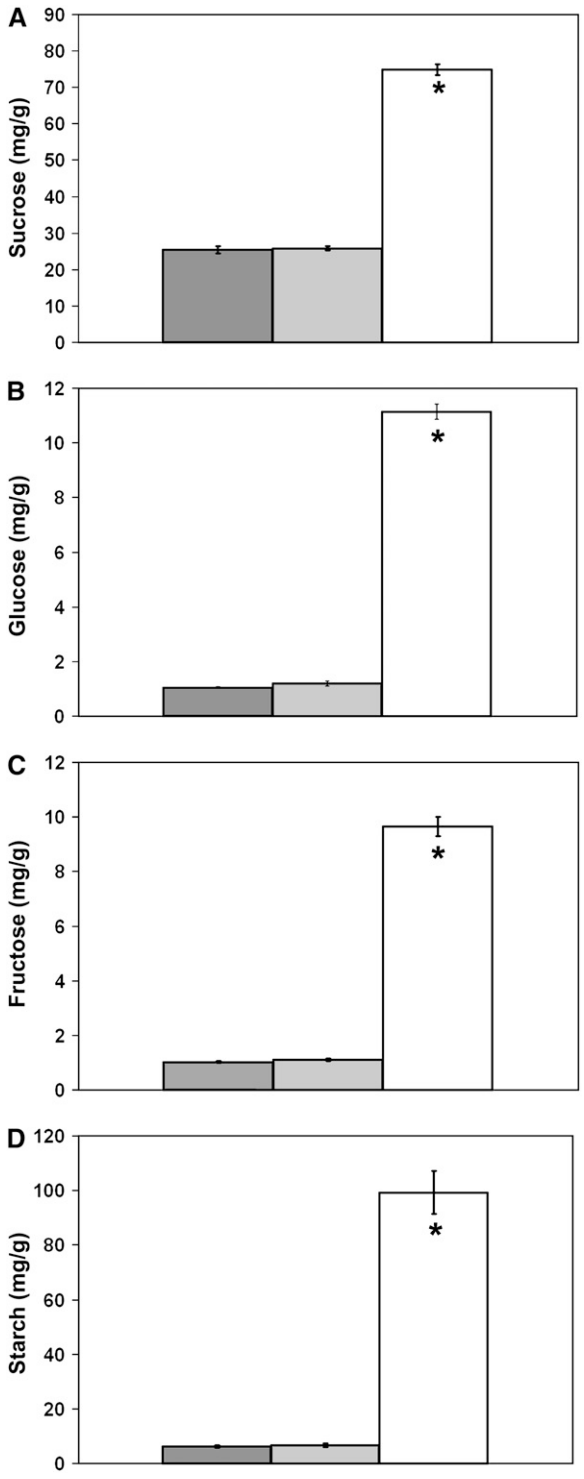

Figure 7. *tdy1* yellow sectors accumulate excess soluble sugars and starch. Bars represent the mean of six samples and error bars represent the SE. Wild type is represented in dark gray, *tdy1* green sectors in light gray, and *tdy1* yellow sectors in white. A, Suc. B, Glc. C, Fru. D, Starch quantification in leaves. An asterisk indicates that the value is significantly different from wild type at $P \leq 0.0001$ using Student's *t* test. Units for each image are mg/g fresh weight.

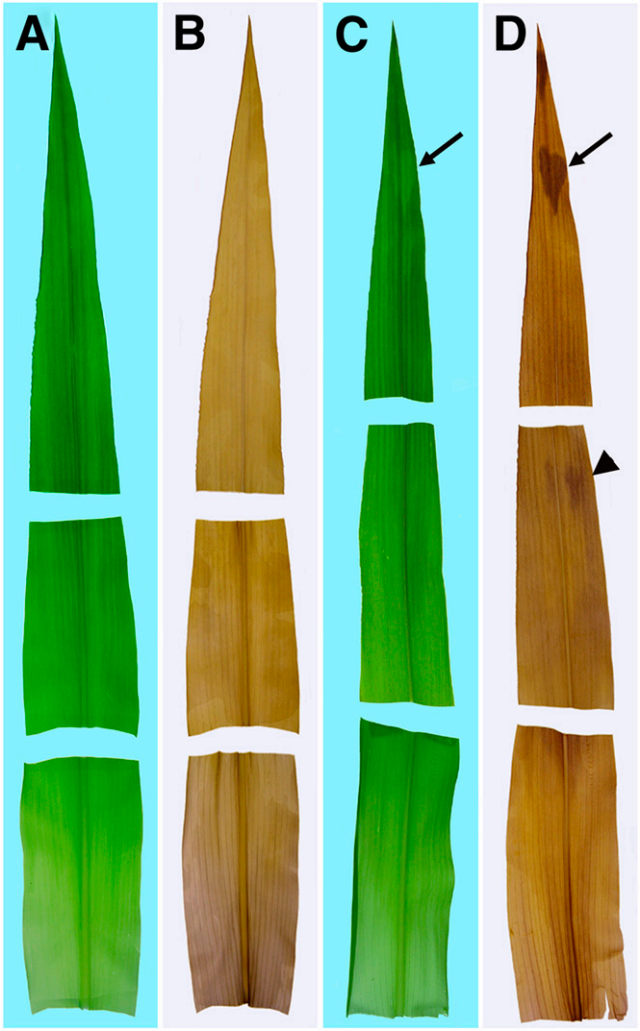

Figure 8. *tdy1* yellow sectors accumulate starch prior to chlorosis. A and B, Wild-type leaf. C and D, *tdy1* leaf. Leaves were divided into thirds corresponding to the tip (oldest), middle, and base (youngest) regions. A and C, Photographs before staining. B and D, Photographs of cleared, IKI-stained leaves. Arrows point to faintly visible yellow sector in mutant leaf tip that accumulates excess starch. Arrowhead indicates region of tissue preferentially accumulating starch prior to chlorosis.

during the summer never form yellow sectors later in development (Fig. 1B).

Sectors first become visible 5 d after the leaf blade completely emerges from the whorl (Fig. 3). Upon emergence, leaf blade tissues are exposed to sufficient light levels to complete chloroplast development and to accumulate high quantities of chlorophylls (Kirchanksi, 1975). Additionally, two other major events occur in leaf development around this time. First, soon after exposure to light, the leaf transitions from a carbon-importing sink tissue to a photosynthetically active, carbon-accumulating and carbon-exporting source tissue (Turgeon, 1989; Evert et al., 1996). Second, development is completed as a basipetal wave of differentiation passes down the leaf and determines cell identity (Sylvester et al., 1990, 1996). These are developmental events that occur once in the lifetime of a leaf and may underlie the timing and irreversibility of *tdy1* sector formation.

The *tdy1* mutant phenotype is evident only in leaf blade tissues. Sectors are not seen in leaf sheaths, stems, husk sheaths, or glumes (Fig. 1D; data not shown). The physiology and anatomy of maize leaf blades differ significantly from these other photosynthetic tissues. With the exception of the first leaf blade, which displays C_3 characteristics, blade tissue utilizes the C_4 carbon assimilation pathway, whereas sheath, husk, glume, and stem tissues all use C_3 carbon assimilation (Crespo et al., 1979; Langdale and Nelson, 1991). Additionally, blade tissue is the principal site of carbon fixation and thereby experiences a much greater osmotic flux compared to C_3 tissues (Hofstra and Nelson, 1969; Evert et al., 1996). Another difference is that the majority of photoassimilate loading into veins occurs in the blade. Whereas some loading does occur in the veins of these other tissues, their vein systems principally function in long-distance transport rather than in loading of assimilates (Fritz et al., 1989). Some of these distinctions may be responsible for why *tdy1* sectors are found only in leaf blades.

Examination of the histology and ultrastructure of *tdy1* yellow sectors revealed striking differences compared to green *tdy1* sectors and wild-type leaves. *tdy1* yellow sectors have greatly reduced photosynthetic membranes in the chloroplasts of mesophyll cells and accumulate excessive starch in both mesophyll and bundle sheath cells. Iodine staining of starch in faintly sectored *tdy1* leaves shows that all photosynthetic cells throughout a sector display the starch accumulation phenotype. Furthermore, starch accumulation precedes visible observation of a yellow sector, suggesting that chlorosis is a secondary consequence of a defect in carbohydrate partitioning. Quantifying the carbohydrate levels in *tdy1* sectors revealed that yellow tissues

Table II. *Photosynthesis rate and gas exchange measurements*

Data represent means of nine samples combined from 3 d ±SE. Units for photosynthesis rate are μmol CO_2 fixed m^{-2} s^{-1} and the units for stomatal conductance measurements are μmol.

Leaf Tissue	Photosynthesis	% of Wild Type	Stomatal Conductance	% of Wild Type
Wild type	28.4 ± 1.3	100	0.089 ± 0.01	100
tdy1 green	24.3 ± 2.4	85.5	0.081 ± 0.02	91.0
tdy1 yellow	4.5[a] ± 0.9	15.8	0.003[a] ± 0.001	3.4

[a]Value is significantly different from wild type at $P < 0.001$ using ANOVA.

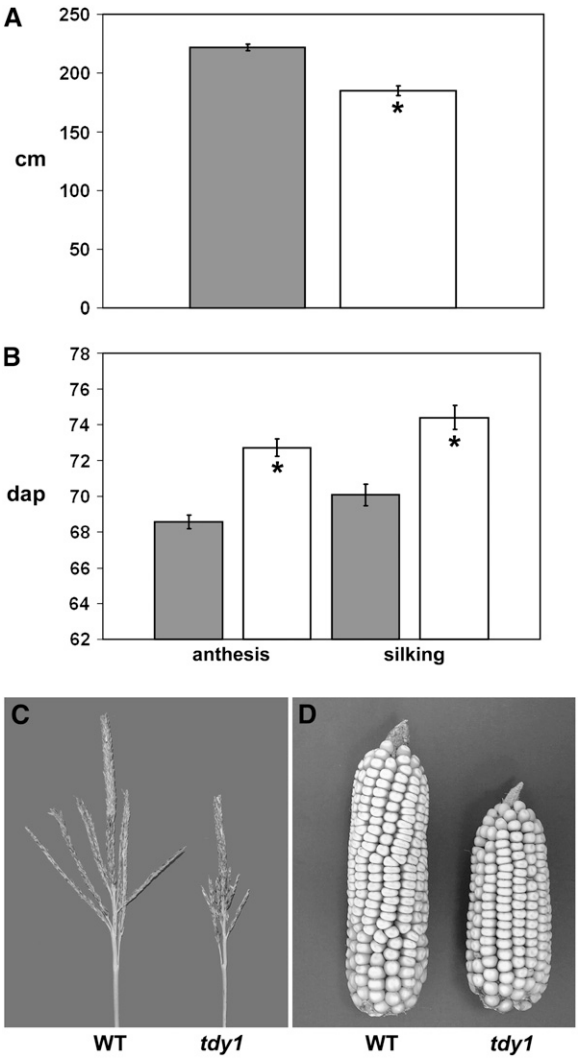

Figure 9. Reduced growth and yield in *tdy1* mutants. Bars represent the mean and error bars represent the SE. Wild type is represented in dark gray and *tdy1* mutants in white. An asterisk indicates that the value is significantly different from wild type at $P < 0.001$ using Student's *t* test. A, *tdy1* mutants have reduced plant height ($n = 13$). Units are centimeters above the soil surface. B, *tdy1* mutants are delayed in flowering. Anthesis is pollen shed ($n = 14$) and silking is silk emergence ($n = 15$). Units are days after planting (dap). C, *tdy1* mutants have reduced tassel size. D, *tdy1* mutants have reduced ear size. WT, Wild type.

accumulate approximately 3- to 16-fold higher levels of Suc, Glc, Fru, and starch compared with *tdy1* green sectors or wild-type leaves. Because Suc is transiently stored during the day in the vacuole, the engorged vacuoles observed in yellow sectors (Fig. 5C) may be at least partly explained by an increased osmotic potential causing water uptake into the vacuoles. Consistent with this, anthocyanins accumulate exclusively in the yellow sectors of *tdy1* leaves. Epidermal cells, the site of anthocyanin accumulation in the leaf blade, are symplastically connected to underlying mesophyll cells. Therefore, they presumably also contain high carbohydrate levels in *tdy1* yellow sectors and likewise experience osmotic stress, which is known to result in anthocyanin accumulation (Chalker-Scott, 1999).

Mesophyll cell chloroplasts do not normally accumulate starch unless plants have experienced severe stress, such as removal of the developing ear or blockage of phloem loading (Allison and Weinmann, 1970; Jeannette et al., 2000). The large quantities of starch in *tdy1* yellow mesophyll cells suggest that these tissues are subjected to a stress similar to that of failing to export fixed carbon. In addition, we observed a significant reduction in plant height, tassel and ear size, and a delay in reproductive maturity in *tdy1* mutants as compared to wild-type siblings. These phenotypes have been reported in plants with reduced levels of photoassimilates available to be transported to growing sinks (Russin et al., 1996; Burkle et al., 1998; Gottwald et al., 2000; Niittyla et al., 2004).

tdy1 yellow sectors have reduced levels of photosynthetic pigments and membranes. However, they remarkably accumulate 300% to 1,600% more carbohydrates than the green sectors of *tdy1* leaves or wild-type siblings. We determined that the yellow sectors have greatly reduced rates of photosynthesis and gas exchange. These data may indicate that yellow sectors are not synthesizing the fixed carbon that accumulates in these tissues, but possibly importing them from neighboring green sectors. One explanation for these data could be that a developmental block occurred in the yellow sectors, causing them to retain sink identity and to continue to import carbon from neighboring green source tissues. This would also explain how high levels of carbohydrates accumulate in the yellow sectors against a steep concentration gradient. Alternatively, it is possible that the reduced rates of photosynthesis in the *tdy1* yellow sectors are sufficient to produce photoassimilates in these tissues and the fixed carbon accumulates to high levels due to reduced capacity to export. In this case, accumulation of excess carbohydrates against the concentration gradient may be mediated by compartmentalization and storage of surplus Suc in the vacuole and starch in the chloroplasts. Future work will test these hypotheses.

Two predominant models have been proposed to explain the formation of sectors in variegated mutants (see Wetzel et al., 1994; Wu et al., 1999; Yu et al., 2004 for discussion). The first model suggests that a partially redundant function can sometimes compensate for the loss-of-function mutation and rescues the phenotype in the green sectors. The second model proposes that a threshold of activity determines sector formation: Exceeding the threshold produces one type of sector and remaining below the threshold produces the other. From our collective observations, we favor the threshold model to explain sector formation in *tdy1* leaves.

Because sectoring requires high light illumination and is evident shortly after blade emergence from the whorl, *tdy1* must function at or prior to this stage of development. We postulate that several nonmutually exclusive mechanisms involving sugar sensing, accumulation, or movement might explain how green and

yellow sectors form in *tdy1* mutant leaves. In yellow sectors, lack of TDY1 function results in failure to export sugar and buildup of carbohydrates in a nonclonal region of tissue. We suggest that high levels of sugars in these cells leads to feedback inhibition of photosynthetic gene expression and chlorophyll synthesis, which in turn lead to reduced chlorophyll accumulation, and ultimately in yellow coloration of the tissue. Reduced photosynthetic pigment levels could result in damage to photosynthetic membranes under high light, causing a decrease in their abundance, and thereby reducing photosynthesis and stomatal conductance rates.

To explain the formation of green tissues in *tdy1* leaves, we propose that sugar levels do not exceed the threshold necessary to trigger formation of a yellow sector. This may occur due to multiple mechanisms (e.g. variation in light levels, more efficient phloem loading, or reduction in sugar levels due to proximity to a yellow sector importing the sugar). Subsequent to the events determining sector identity, cells of both tissue types differentiate and assume their final fate. After this time, TDY1 function is no longer required and cell fate is determined. Hence, we propose that *tdy1* green tissue fails to exceed the threshold required to trigger sector formation and differentiates as normal functioning tissue escaping the consequences of the mutation. This is consistent with the fact that we observed no significant differences between *tdy1* green tissue and wild-type tissue.

A speculative function of TDY1 consistent with this model for variegation is as a sugar flux or osmotic stress sensor, which activates an export pathway under high sugar conditions. For example, TDY1 may control induction of a high capacity sugar transporter responsible for loading Suc into the phloem (Weise et al., 2000). Differential induction of a transporter could explain both types of sector formation. In the absence of *tdy1* function, under circumstances when sugar concentrations in cells are low, there is no need to activate the inducible export pathway and no consequence to the defect. However, when sugar concentrations are high, the absence of TDY1 prevents activation of the inducible export pathway. The resulting buildup of photoassimilates diffuses both laterally and longitudinally through a nonclonal region of tissue, causing formation of a *tdy1* yellow sector and terminal identity as carbon-accumulating tissue. This proposed function of TDY1 does not require a redundant function to explain the formation of green tissue in *tdy1* mutant leaves, simply a sugar concentration below the threshold necessary to induce the export pathway.

Our characterization of the *tdy1* variegation and carbohydrate accumulation phenotypes has identified a novel pathway regulating sugar export from leaves. To our knowledge, no other mutant with this particular set of defects has been described. Other starch-accumulating mutants have been characterized, but they function in the starch catabolic pathway and affect the entire leaf (Zeeman et al., 1998; Critchley et al., 2001; Yu et al., 2001; Dinges et al., 2003; Niittyla et al., 2004). Similarly, antisense expression or mutation of Suc transporters results in starch accumulation in leaves, but likewise affects the entire organ (Riesmeier et al., 1994; Burkle et al., 1998; Gottwald et al., 2000). Several variegated mutants have been characterized in dicots, but none have been reported to preferentially accumulate high levels of sugars and starch. The only characterized mutant with a resemblance to *tdy1* is *sucrose export defective1* (*sxd1*) in maize (Russin et al., 1996; Provencher et al., 2001). *sxd1* mutants develop sectors at the tip of the leaf blade that accumulate high levels of sugars, starch, and anthocyanins. However, the temporal appearance and pattern of sectors between the two mutants are quite distinct. *sxd1* sectors progressively spread basipetally over the lifetime of the mature leaf. To our knowledge, these are the only two mutants that possess a nonclonal variegation pattern with differential carbohydrate accumulation, so it will be insightful to determine whether *tdy1* and *sxd1* function in the same genetic pathway or regulate carbohydrate accumulation in leaves via different mechanisms. Future work will elucidate how *tdy1* coordinates development among nonclonally related cells and the genetic pathways regulating carbohydrate partitioning in maize leaves.

MATERIALS AND METHODS

Plant Materials and Growth Conditions

Plants were grown in the summer nurseries at the Bay Area Research and Extension Center, University of California at Berkeley (San Jose, CA), and at the Rock Springs Agronomy Farm, Pennsylvania State University (State College, PA). For photosynthesis and stomatal conductance measurements, plants were grown in the summer nursery in Johnston, IA. Plants grown in the greenhouse and growth chamber were supplemented with sodium vapor and mercury halide lamps at 1,400 (high) or 75 (low) μmol m^{-2} s^{-1} light under a 12-h d (30°C)/12-h night (20°C) cycle. For the constant high light experiment, plants were grown in a high light growth chamber under 24-h constant light with a constant temperature of 28°C. For the visible sector time-course experiments, *tdy1*-segregating families were grown in the greenhouse and newly emerged fourth leaves were observed throughout their development.

Genetic Stocks

Maize (*Zea mays*) EMS-mutagenized F_2 families were obtained from J. Hollick (University of California, Berkeley, CA). These populations were derived from mutagenizing pollen from stock 611A obtained from the Maize Genetics Cooperation Stock Center as described by Hollick and Chandler (2001). The anthocyanin-accumulating genetic line is a W23-derived stock containing structural and regulatory alleles necessary for anthocyanin expression in leaves (see Hollick and Chandler, 2001 for description). B73 inbred seed was provided by Pioneer Hi-Bred. The *tdy1-Reference* (*tdy1-R*; hereafter *tdy1*) mutation was introgressed into the B73 genetic background three or more times prior to analyses, except in the experiments performed using the anthocyanin-accumulating background. B-A translocation stocks were obtained from M. Scanlon (Cornell University, Ithaca, NY). *tdy1* was crossed to inbreds B73, Mo17, and W23, and F_1 plants self fertilized to create segregating F_2 families used for molecular fine mapping.

Pigment Analyses

Chlorophyll and total carotenoid concentrations were quantified according to Lichtenthaler and Wellburn (1983). Leaf discs of field-grown mature leaf tissues were harvested with an 11-mm-diameter cork borer, weighed, frozen in liquid nitrogen, ground to a fine powder in a mortar and pestle, and extracted

in acetone. For *tdy1* leaves, samples were collected from the center of large green or yellow sectors to avoid border regions. Samples were kept on ice in the dark during processing. Extracts were gently rotated at 4°C in the dark for 1 h. Cell debris was removed by centrifugation and the supernatant assayed for pigment concentrations. For each tissue type (*tdy1* yellow, *tdy1* green, and wild type), 12 different samples were measured. The experiment was performed three times.

Fluorescent and Electron Microscopy

For cytological studies, samples were isolated from mature, field-grown leaves collected at the end of the day. Tissues for leaf histology were processed according to Inada et al. (1998). Briefly, small segments of fresh leaf blade tissue, approximately 2 × 2 mm, were fixed at 4°C overnight in 4% paraformaldehyde buffered with 20 mM sodium cacodylate, pH 7.5, dehydrated in a graded ethanol series, and embedded in Technovit 7100. Thin sections of approximately 1 μm were made with an Ultramicrotome (RMC MT6000; RMC) and stained with 100 μg mL^{-1} $DiOC_7$ in ethanol. Sections were observed under blue light with a Zeiss Axiophot fluorescent microscope. Additionally, free-hand sections were examined under bright-field and UV illumination using a Nikon Eclipse 80i fluorescent microscope.

To analyze chloroplast ultrastructure, samples were prepared for TEM analysis. In the initial step, segments of leaf blades were dissected with a sharp razor blade and immediately placed into 5% glutaraldehyde, 50 mM sodium cacodylate buffer, pH 7.2, on ice. The remainder of tissue preparation was performed under vacuum using a Pelco 3451 laboratory microwave system (Ted Pella). Tissues were fixed for 4 min, rinsed with 50 mM sodium cacodylate, pH 7.2, for 40 s three times, postfixed in 1% osmium tetroxide for 4 min, and rinsed with water for 40 s three times. Tissues were dehydrated through a graded acetone series (each 40 s twice) and infiltrated with Spurr's epoxy resin (4 min each step; Spurr, 1969). All of the above steps took place at 45°C. Power settings were 1 for fixation and dehydration steps, 2 for the first infiltration step (acetone:resin [2:1]), 3 for the second infiltration step (acetone: resin [1:1]), and 4 for the rest of steps. Ultrathin sections of approximately 100 nm were cut with a glass knife on an ultramicrotome, lifted on to glow-discharged carbon-coated copper grids stained with 0.5% formvar, and observed at 80 kV on a FEI Tecnai 12 transmission electron microscope.

Carbohydrate Quantification

Soluble sugar (Suc, Glc, and Fru) and starch quantities were determined using commercial assay kits according to the manufacturer's instructions (R-Biopharm) as described (Dinges et al., 2003). Mature, adult leaves were collected on three different days from field-grown plants at the end of the photoperiod and six samples were measured for each tissue. The experiment was repeated three times.

To visualize starch in leaf tissues, leaves of wild-type and *tdy1* mutants were collected as above, decolorized in boiling 95% ethanol, and stained with IKI according to Ruzin (1999). To visualize starch prior to observing chlorotic sectors, leaf 10 from greenhouse-grown plants was harvested when the base of the leaf blade was emerging from the whorl, divided into thirds, and similarly analyzed.

Photosynthesis and Stomatal Conductance Measurements

Measurements were taken on adult, fully expanded leaves in midsummer between 1 PM and 3 PM using a LICOR LI-6400 open photosynthesis system. As part of a randomized design, plants were grown in three separate replicate plots. The device maintained the following conditions throughout the assays: an artificial light source with an intensity of 1,800 μmol photosynthetically active radiation m^{-2} s^{-1}, leaf temperature of 34°C to 35°C, CO_2 concentration of 400 μL L^{-1}, air flow of 500 μmol, and relative humidity of 58% to 64%. Three samples were assayed for each tissue type on three different days. Data presented in Table II are a combined analysis because no differences between the datasets were found, whether compared for a particular day or across all dates. Individual day data are found in Supplemental Table S3.

Morphometric Analyses

For morphometric studies, measurements were made from at least two F_2 families with ≥30 individuals and segregating wild type and *tdy1* in a 1:1 fashion. Representative data from one family are shown. Plant height was measured from the surface of the soil to the tip of the central spike of the tassel (n = 13). Tassel height was measured from the node of the topmost leaf to the tip of the central spike (n = 18). Anthesis date was recorded as the day of first pollen shed (n = 14). Similarly, silking date was the date of first silk emergence (n = 15). Ear length was measured from the base of the bottom row of kernels to the tip of the ear (n = 12). Kernel weight was determined as the average of 100 randomly selected F3 kernels per ear (n = 12).

Statistical Analyses

For photosynthetic pigment quantifications, carbohydrate measurements, and the morphometric analyses, statistical significance was determined using Student's two-tailed t test. For photosynthesis and stomatal conductance assays, statistical significance was determined using ANOVA (SAS). Data from each day and combined across all three days showed the same Duncan's groupings.

Supplemental Data

The following materials are available in the online version of this article.

Supplemental Table S1. Photosynthetic pigment quantification for all replicates.

Supplemental Table S2. Sugars and starch quantification for all replicates.

Supplemental Table S3. Photosynthesis and stomatal conductance data for all replicates.

Supplemental Figure S1. Wild-type and *tdy1* leaves grown under constant high light.

Supplemental Figure S2. Reduced tassel phenotypes in *tdy1* mutants.

Supplemental Figure S3. Reduced ear length and kernel weight in *tdy1* mutants.

ACKNOWLEDGMENTS

We thank Tony Omeis, Barbara Rotz, Scott Harkam, and Bob Oberheim for excellent plant care. We are grateful to Chris Zinselmeier and Sharon Cerwick for assistance with the photosynthesis measurements and statistical analyses. We thank Jay Hollick for the gift of the EMS-mutagenized families and Mike Scanlon for the B-A translocation stocks. We are also grateful to two anonymous reviewers for their suggestions and to Simon Gilroy and members of the Braun and McSteen labs for critical reading of the manuscript and discussions of the data. Early work on this project was performed in the Freeling laboratory (funded by National Institutes of Health grant no. GM42610 and the University of California Agricultural Experiment Station).

Received September 26, 2006; accepted October 17, 2006; published October 27, 2006.

LITERATURE CITED

Allison JCS, Weinmann H (1970) Effect of absence of developing grain on carbohydrate content and senescence of maize leaves. Plant Physiol **46:** 435–436

Beckett JB (1994) Locating recessive genes to chromosome arm with B-A translocations. *In* M Freeling, V Walbot, eds, The Maize Handbook. Springer-Verlag, New York, pp 315–327

Brutnell TP, Sawers RJH, Mant A, Langdale JA (1999) BUNDLE SHEATH DEFECTIVE2, a novel protein required for post-translational regulation of the *rbcL* gene of maize. Plant Cell **11:** 849–864

Burkle L, Hibberd JM, Quick WP, Kuhn C, Hirner B, Frommer WB (1998) The H+-sucrose cotransporter NtSUT1 is essential for sugar export from tobacco leaves. Plant Physiol **118:** 59–68

Chalker-Scott L (1999) Environmental significance of anthocyanins in plant stress responses. Photochem Photobiol **70:** 1–9

Chatterjee M, Sparvoli S, Edmunds C, Garosi P, Findlay K, Martin C (1996) DAG, a gene required for chloroplast differentiation and palisade development in *Antirrhinum majus*. EMBO J **15:** 4194–4207

Crespo H, Frean M, Cresswell C, Tew J (1979) The occurrence of both C_3 and C_4 photosynthetic characteristics in a single *Zea mays* plant. Planta **147:** 257–263

Critchley JH, Zeeman SC, Takaha T, Smith AM, Smith SM (2001) A critical role for disproportionating enzyme in starch breakdown is revealed by a knock-out mutation in *Arabidopsis*. Plant J **26:** 89–100

Dinges JR, Colleoni C, James MG, Myers AM (2003) Mutational analysis of the pullulanase-type debranching enzyme of maize indicates multiple functions in starch metabolism. Plant Cell **15:** 666–680

Esau K (1977) Anatomy of Seed Plants, Ed 2. John Wiley and Sons, New York

Evert RF, Russin WA, Bosabalidis AM (1996) Anatomical and ultrastructural changes associated with sink-to-source transition in developing maize leaves. Int J Plant Sci **157:** 247–261

Freeling M (1992) A conceptual framework for maize leaf development. Dev Biol **153:** 44–58

Fritz E, Evert RF, Nasse H (1989) Loading and transport of assimilates in different maize leaf bundles—digital image analysis of ^{14}C microautoradiographs. Planta **178:** 1–9

Gottwald JR, Krysan PJ, Young JC, Evert RF, Sussman MR (2000) Genetic evidence for the *in planta* role of phloem-specific plasma membrane sucrose transporters. Proc Natl Acad Sci USA **97:** 13979–13984

Hall LN, Langdale JA (1996) Molecular genetics of cellular differentiation in leaves. New Phytol **132:** 533–553

Hall LN, Rossini L, Cribb L, Langdale JA (1998) GOLDEN 2: a novel transcriptional regulator of cellular differentiation in the maize leaf. Plant Cell **10:** 925–936

Hofstra G, Nelson C (1969) The translocation of photosynthetically assimilated ^{14}C in corn. Can J Bot **47:** 1435–1442

Hollick J, Chandler V (2001) Genetic factors required to maintain repression of a paramutagenic maize *pl1* allele. Genetics **157:** 369–378

Inada N, Sakai A, Kuroiwa H, Kuroiwa T (1998) Three-dimensional analysis of the senescence program in rice (*Oryza sativa* L.) coleoptiles: investigations of tissues and cells by fluorescence microscopy. Planta **205:** 153–164

Jankovsky JP, Smith LG, Nelson T (2001) Specification of bundle sheath cell fates during maize leaf development: roles of lineage and positional information evaluated through analysis of the *tangled1* mutant. Development **128:** 2747–2753

Jeannette E, Reyss A, Gregory N, Gantet P, Prioul JL (2000) Carbohydrate metabolism in a heat-girdled maize source leaf. Plant Cell Environ **23:** 61–69

Kaiser G, Heber U (1984) Sucrose transport into vacuoles isolated from barley mesophyll protoplasts. Planta **161:** 562–568

Keddie JS, Carroll B, Jones JDG, Gruissem W (1996) The DCL gene of tomato is required for chloroplast development and palisade cell morphogenesis in leaves. EMBO J **15:** 4208–4217

Kessler S, Seiki S, Sinha N (2002) *Xcl1* causes delayed oblique periclinal cell divisions in developing maize leaves, leading to cellular differentiation by lineage instead of position. Development **129:** 1859–1869

Kirchanksi SJ (1975) The ultrastructural development of the dimorphic plastids of *Zea mays* L. Am J Bot **62:** 695–705

Langdale JA, Kidner CA (1994) *bundle sheath defective*, a mutation that disrupts cellular differentiation in maize leaves. Development **120:** 673–681

Langdale JA, Nelson T (1991) Spatial regulation of photosynthetic development in C_4 plants. Trends Genet **7:** 191–196

Lichtenthaler HK, Wellburn AR (1983) Determinations of total carotenoids and chlorophylls *a* and *b* of leaf extracts in different solvents. Biochem Soc Trans **11:** 591–592

Muller HJ (1932) Further studies on the nature and causes of gene mutations. *In* DF Jones, ed, Proceedings of the 6th International Congress of Genetics. Brooklyn Botanic Gardens, Menasha, WI, pp 213–255

Niittyla T, Messerli G, Trevisan M, Chen J, Smith AM, Zeeman SC (2004) A previously unknown maltose transporter essential for starch degradation in leaves. Science **303:** 87–89

Poethig RS (1984) Cellular parameters of leaf morphogenesis in maize and tobacco. *In* RA White, WC Dickison, eds, Contemporary Problems in Plant Anatomy. Academic Press, New York, pp 235–259

Poethig RS, Szymkowiak EJ (1995) Clonal analysis of leaf development in maize. Maydica **40:** 67–76

Provencher LM, Miao L, Sinha N, Lucas WJ (2001) *Sucrose export defective1* encodes a novel protein implicated in chloroplast-to-nucleus signaling. Plant Cell **13:** 1127–1141

Rhoades M, Carvalho A (1944) The function and structure of the parenchyma sheath plastids of the maize leaf. Bull Torrey Bot Club **71:** 335–346

Riesmeier JW, Willmitzer L, Frommer WB (1994) Evidence for an essential role of the sucrose transporter in phloem loading and assimilate partitioning. EMBO J **13:** 1–7

Rodermel S (2002) Arabidopsis variegation mutants. *In* C Somerville, E Meyerowitz, eds, The Arabidopsis Book. American Society of Plant Biologists, Rockville, MD, pp 1–33

Roth R, Hall LN, Brutnell TP, Langdale JA (1996) *bundle sheath defective2*, a mutation that disrupts the coordinated development of bundle sheath and mesophyll cells in the maize leaf. Plant Cell **8:** 915–927

Russin WA, Evert RF, Vanderveer PJ, Sharkey TD, Briggs SP (1996) Modification of a specific class of plasmodesmata and loss of sucrose export ability in the *sucrose export defective1* maize mutant. Plant Cell **8:** 645–658

Ruzin S (1999) Plant Microtechnique and Microscopy. Oxford University Press, New York

Sestak Z (1963) Changes in the chlorophyll content as related to photosynthetic activity and age of leaves. Photochem Photobiol **2:** 101–110

Sheen J (1990) Metabolic repression of transcription in higher plants. Plant Cell **2:** 1027–1038

Spurr A (1969) A low-viscosity epoxy resin embedding medium for electron microscopy. J Ultrastruct Res **26:** 31–43

Sylvester AW, Cande WZ, Freeling M (1990) Division and differentiation during normal and *liguleless1* maize leaf development. Development **110:** 985–1000

Sylvester AW, Smith L, Freeling M (1996) Acquisition of identity in the developing leaf. Annu Rev Cell Dev Biol **12:** 257–304

Turgeon R (1989) The sink-source transition in leaves. Annu Rev Plant Physiol Plant Mol Biol **40:** 119–138

Wang Q, Sullivan RW, Kight A, Henry RL, Huang JR, Jones AM, Korth KL (2004) Deletion of the chloroplast-localized *Thylakoid formation1* gene product in Arabidopsis leads to deficient thylakoid formation and variegated leaves. Plant Physiol **136:** 3594–3604

Weise A, Barker L, Kuhn C, Lalonde S, Buschmann H, Frommer WB, Ward JM (2000) A new subfamily of sucrose transporters, SUT4, with low affinity/high capacity localized in enucleate sieve elements of plants. Plant Cell **12:** 1345–1355

Wetzel CM, Jiang CZ, Meehan LJ, Voytas DF, Rodermel SR (1994) Nuclear-organelle interactions: the *immutans* variegation mutant of *Arabidopsis* is plastid autonomous and impaired in carotenoid biosynthesis. Plant J **6:** 161–175

Wu DY, Wright DA, Wetzel C, Voytas DF, Rodermel S (1999) The *immutans* variegation locus of Arabidopsis defines a mitochondrial alternative oxidase homolog that functions during early chloroplast biogenesis. Plant Cell **11:** 43–55

Yu F, Park S, Rodermel S (2004) The Arabidopsis FtsH metalloprotease gene family: interchangeability of subunits in chloroplast oligomeric complexes. Plant J **37:** 864–876

Yu TS, Kofler H, Hausler RE, Hille D, Flugge UI, Zeeman SC, Smith AM, Kossmann J, Lloyd J, Ritte G, et al (2001) The Arabidopsis *sex1* mutant is defective in the R1 protein, a general regulator of starch degradation in plants, and not in the chloroplast hexose transporter. Plant Cell **13:** 1907–1918

Zeeman SC, Northrop F, Smith AM, Rees T (1998) A starch-accumulating mutant of *Arabidopsis thaliana* deficient in a chloroplastic starch-hydrolysing enzyme. Plant J **15:** 357–365